JOURNAL OF SOLID STATE CHEMISTRY 118, 357–366 (1995)

Ferrite $Bi_{13}Ba_2Sr_{25}Fe_{13}O_{66}$: A Double Collapsed Structure Derived from the "2201–0201" Intergrowth $Bi_2Sr_4Fe_2O_{10}$

M. Hervieu,* M. T. Caldes,† C. Michel,* D. Pelloquin,* and B. Raveau*

*Laboratoire de Cristallographie et Sciences des Matériaux, ISMRA-Université de Caen, Bd du maréchal Juin, 14050 Caen Cedex, France; and †Instituto de Ciencia de Materiales de Barcelona (CSIC), Campus UAB, 08913 Bellaterra, Barcelona, Spain

Received December 6, 1994; accepted March 15, 1995

A new ferrite, $Bi_{13}Ba_2Sr_{25}Fe_{13}O_{66}$, has been synthesized. It crystallizes in the space group $C2/c$ with $a = 39.108$ (5) Å, $b = 5.4371$ (5) Å, $c = 37.223$ (5) Å, $\beta = 114.9°$ (1). A structural model has been established, using high-resolution electron microscopy. It can be described as a double collapsed structure derived from the "2201–0201" intergrowth $Bi_2Sr_4Fe_2O_{10}$. Another description of this structure is presented: it consists of stair-like Bi_2O_2 layers parallel to (001) intergrown with K_2NiF_4-type layers. The stairs that form the bismuth oxygen layers are 7 bismuth atoms wide, whereas the K_2NiF_4 layers are 13 FeO_6 octahedra thick, so that this structure can be considered as the "$m = 7$, $n = 13$" members of a very promising series of ferrites $(Bi_{2-x}Ba_xO_2)_m(Sr_{2-x}Ba_xFeO_4)_n$. Extended defects involving longitudinal intergrowth of two m and m' members are observed, as well as antiphase boundaries and "SrO" intergrowths.

INTRODUCTION

Recent investigations of the bismuth-based ferrites have shown their great structural similarity with the superconducting layered cuprates. With the discovery of the ferrite $BiPbSr_2FeO_6$ (1), which is isotypic with the 2201 cuprate $Bi_2Sr_2CuO_6$ (2, 3), two ferrites $Bi_2Sr_3Fe_2O_9$ (4) and $Bi_2Sr_4Fe_3O_{12}$ (5) have been synthesized. These two are closely related to the 2212 structure of $Bi_2Sr_2CaCu_2O_8$ (6, 7) and to the 2223 structure of $Bi_{2-x}Pb_xSr_2Ca_2Cu_3O_{10}$ (8), respectively. They differ from the corresponding cuprates by the nature of the iron layers that are double octahedral layers for $Bi_2Sr_3Fe_2O_9$ instead of double pyramidal copper layers for $Bi_2Sr_2CaCu_2O_8$ and triple octahedral layers for $Bi_2Sr_4Fe_3O_{12}$ instead of single square planar layers sandwiched by pyramidal layers in $Bi_{2-x}Pb_xSr_2Ca_2Cu_3O_{10}$. Very recently, a series of intergrowths of the 2201 and 0201 structures, with the ideal formula $Bi_{n+1}Sr_{2n+2}Ba_{n-1}Fe_{n+1}O_{6n+4}$ (9), has been evidenced. The first member of the series $Bi_2Sr_4Fe_2O_{10}$ corresponds to the intergrowth of single 2201 ($Bi_2Sr_2CuO_6$-type) layers with single 0201 (K_2NiF_4-type) layers. The other two members $Bi_3BaSr_6Fe_3O_{16}$ ($n = 2$) and $Bi_4Ba_2Sr_8Fe_4O_{22}$ ($n = 3$), which consist of double and triple 2201-type layers, respectively, open the route to the discovery of new ferrites, owing to the fact that the presence of barium on the bismuth sites appears to be a key factor for their stabilization.

Contrary to the bismuth cuprates, which exhibit collapsed phases derived from the 2201 structure, such as $Bi_{4+x}Sr_7Ba_7Cu_{7-x}O_{42+x/2}$ (10) and $Bi_6Ba_4Cu_2O_{15}$ (11), no shearing phenomena have been obtained at present for bismuth ferrites in spite of the great similarity of the two systems. Taking into consideration the fact that barium seems to be favorable to the formation of such phases, the synthesis of barium-doped bismuth ferrites with compositions close to that of the 0201–2201 intergrowth $Bi_2Sr_4Fe_2O_{10}$ has been investigated. The present paper reports on a new ferrite $Bi_{13}Ba_2Sr_{25}Fe_{13}O_{66}$, which derives from the $Bi_2Sr_4Fe_2O_{10}$ structure by a collapsing mechanism.

EXPERIMENTAL

In order to synthesize the collapsed phase derived from $Bi_2Sr_4Fe_2O_{10}$, the compositions $(Bi, Ba)_{2\pm x}Sr_{4\pm y}Fe_{2-z}O_t$ were investigated for x, y, and z ranging from 0 to 1 by steps of 0.1 and for different Bi/Ba ratios (ranging from 20 to 5). This exploration was based on our previous studies of the collapsed cuprates (10, 11) that indicate that a copper deficiency with respect to the mother structure is necessary to stabilize such phases.

The samples were prepared from mixtures of Bi_2O_3, BaO, $SrCO_3$, and Fe_2O_3, heated at 930°C for 5 days in a nitrogen flow.

The X-ray diffraction (XRD) patterns were registered using a Seifert diffractometer equipped with a primary monochromator in order to select the $CuK\alpha_1$ radiation. Data were collected by step scanning with increments of 0.02° (2θ) in the range $3° < 2\theta < 80°$. Lattice constants were determined using the profile refinement computer program FULLPROF [12], and the pattern-matching option. The electron diffraction (ED) study was performed with a JEOL 200 CX electron microscope fitted with a eucentric goniometer (±60°). The high-resolution electron microscopy (HREM) was performed with a TOPCON

0022-4596/95 $12.00

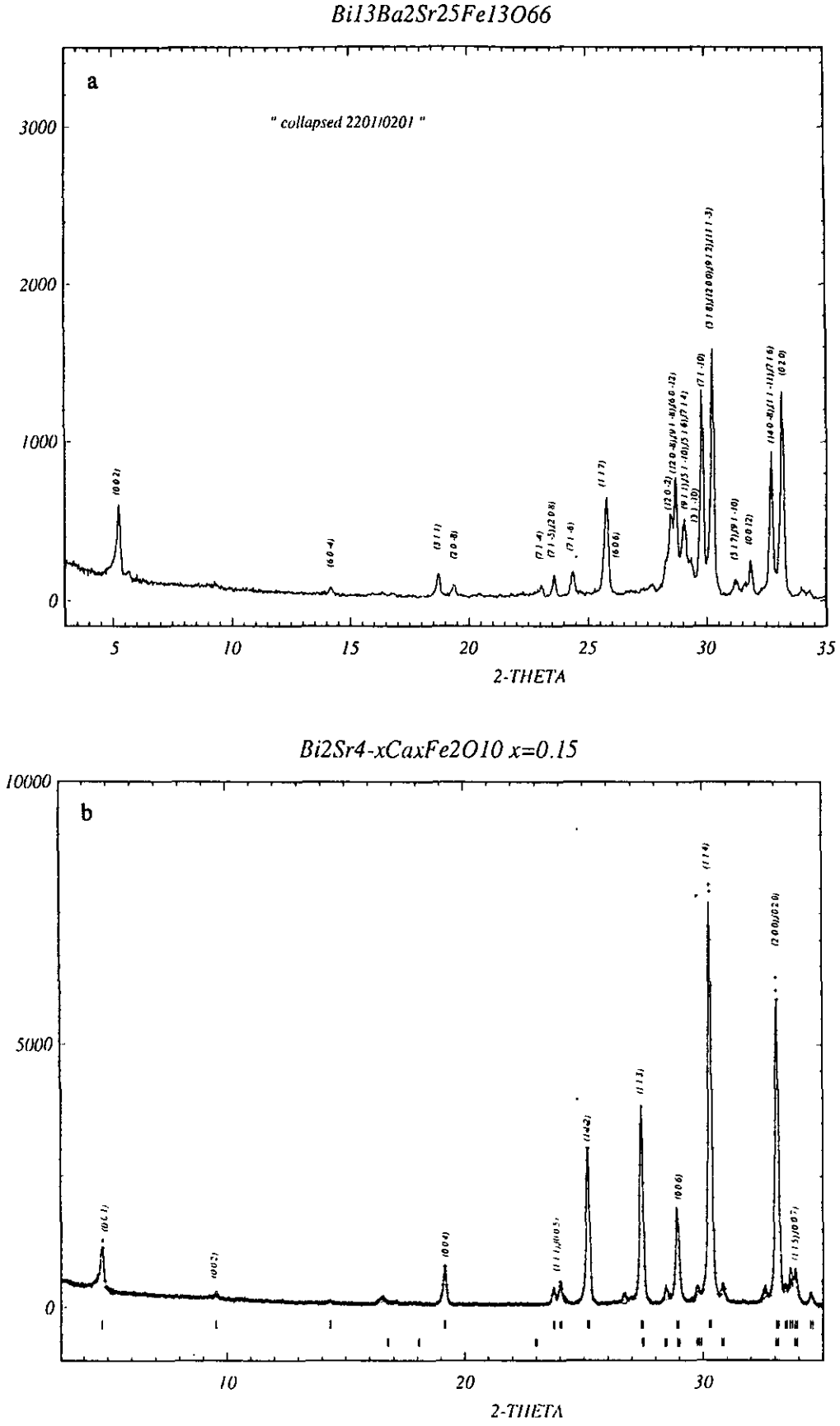

FIG. 1. Powder X-ray patterns of (a) $Bi_{13}Ba_2Sr_{25}Fe_{13}O_{66}$ and (b) $Bi_2Sr_4Fe_2O_{10}$.

002B microscope, operating at 200 kV, having a point resolution of 1.8 Å. The samples were prepared by a smooth crushing in alcohol and the grains were deposited on a holey carbon film. Both microscopes are equipped with a KEVEX analyzer; EDX analyses were systematically made, with $Bi_2Sr_2CuO_6$, $BaCuO_2$, Sr_2CuO_3, and $Sr_2Fe_2O_5$ as standards.

RESULTS AND DISCUSSION

The Double Collapsed Structure of $Bi_{13}Ba_2Sr_{25}Fe_{13}O_{66}$

The EDX analysis performed on many crystals allows the composition of the new phase to be established in connection with the crystallographic observations, as $Bi_{13}Ba_2Sr_{25}Fe_{13}O_{66\pm\delta}$. For this nominal composition, the powder XRD pattern (Fig. 1a) shows that it corresponds to a nearly pure phase and that there exist strong similarities with the pattern of the mother structure $Bi_2Sr_4Fe_2O_{10}$ (9) (Fig. 1b). This is confirmed by ED study and the reconstruction of the reciprocal space evidences a monoclinic cell with $a \approx 39$ Å, $b \approx 5.4$ Å ($\approx a_p\sqrt{2}$), and $c \approx 37.2$ Å ($\approx 2\ \mathbf{c}_{2201/0201}$) and $\beta \approx 115°$, (Fig. 2). The conditions of reflection involve a $C2/c$ space group. The cell parameters were refined from XRD data to the following values:

$$a = 39.108(5)\text{ Å}, \quad b = 5.4371(5)\text{ Å},$$
$$c = 37.223(5)\text{ Å}, \quad \text{and} \quad \beta = 114.9°(1).$$

The value of the c parameter is clearly twice that of the mother phase $Bi_2Sr_4Fe_2O_{10}$, whereas the b parameter ($\approx a_p\sqrt{2}$) is that systematically observed in the layered bismuth oxides. On the opposite, the periodicity along $\vec{a}$ is not directly related to other layered cuprates and ferrites; referring to other collapsed phases, it would depend on the distance between the crystallographic collapsing planes (CCP); in that new phase, a $\sin\beta \approx 7 \times a_p\sqrt{2}$ suggests that the event arises every seven octahedra and the monoclinic symmetry is in favor of a collapsing operation.

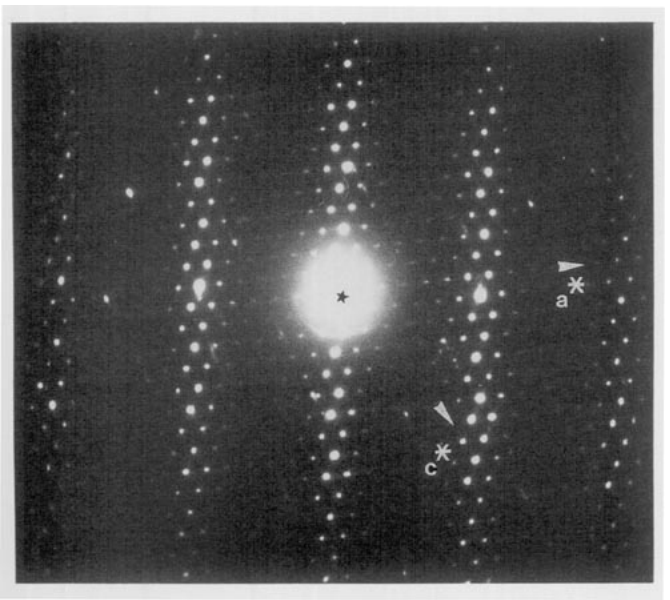

FIG. 2. [010] ED pattern of $Bi_{13}Ba_2Sr_{25}Fe_{13}O_{66}$.

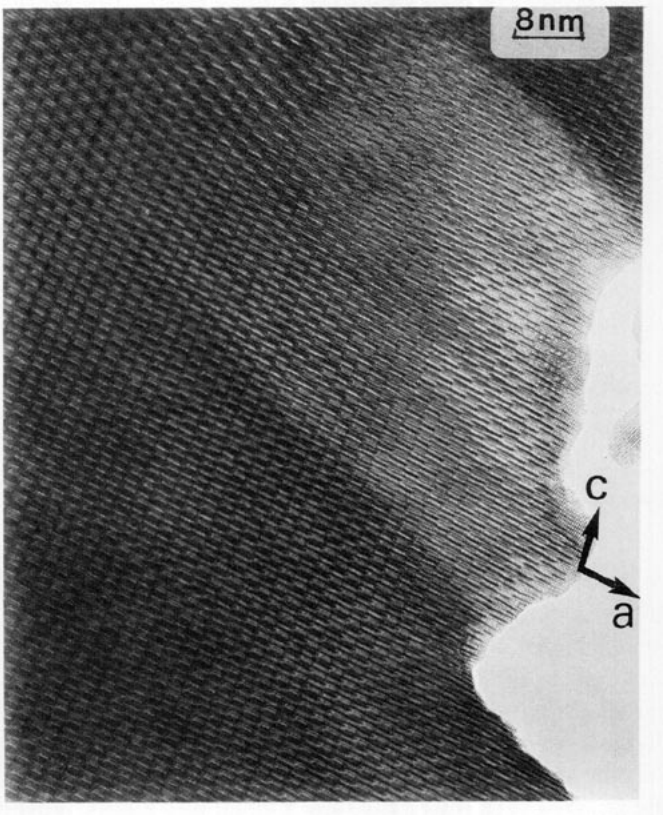

FIG. 3. [010] overall image of $Bi_{13}Ba_2Sr_{25}Fe_{13}O_{66}$: ribbons parallel to (100) are characteristic of the collapsed structures.

The HREM overall images (Fig. 3) confirm the existence of ribbons running along c, characteristic of the collapsed structures (10, 11); the enlarged images allows one to understand the way the layers are shifted and connected. The interpretation can be made easily from the experimental and calculated images of the mother structure $(Bi_2Sr_4FeO_6)^{2201}$ $(Sr_2FeO_4)^{0201}$ (9). An example is shown in Fig. 4, where the positions of the heavy cations are highlighted ($\Delta f \approx -500$ Å): the bright dots are correlated to the Bi, Ba, and Sr positions. The oval-shaped segments of the double Bi rows are easily identified; they are seven octahedra wide. The rows are parallel to [100], i.e., to the $\mathbf{a}_{2201/0201}$ axis of the mother structure, $Bi_2Sr_4Fe_2O_{10}$.

The structure of $Bi_{13}Ba_2Sr_{25}Fe_{13}O_{66}$ can be deduced easily from that of $Bi_2Sr_4Fe_2O_{10}$ by simply considering the relative positions of the oval-shaped segments corresponding to these double "BiO" tapes that are seven bismuth atoms wide along $\mathbf{a}_{2201/0201}$ in both structures (Fig.

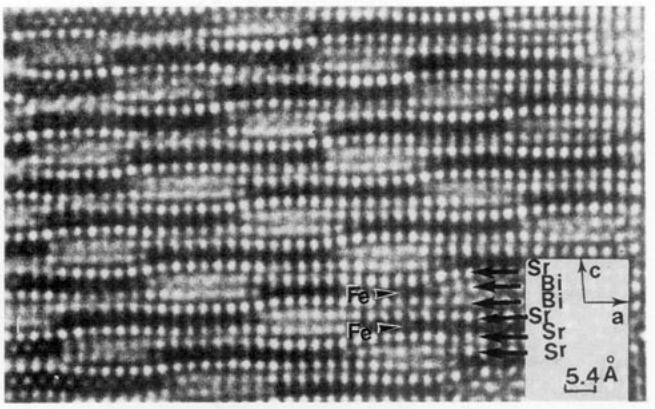

FIG. 4. [010] enlarged image; the bright dots are correlated to the heavy cation positions. The nature of the layers stacked along c is marked in the right part of the micrograph.

5). In the mother structure, $Bi_2Sr_4Fe_2O_{10}$, the oval-shaped bismuth tapes form columns running along $\mathbf{c}_{2201/0201}$ are seven bismuth atoms wide (Fig. 5a), whereas in $Bi_{13}Ba_2Sr_{25}Fe_{13}O_{66}$ the columns of oval-shaped bismuth tapes are no longer parallel to $\mathbf{c}_{2201/0201}$ but are parallel to $\mathbf{c}$ (Fig. 5c). In fact, the configuration of the bismuth oval-shaped tapes of this new structure can be deduced from that of $Bi_2Sr_4Fe_2O_{10}$ by operating a two-step translation. A first translation $\vec{t}_c$ along $\mathbf{c}_{2201/0201}$ of 6.9 Å of two adjacent columns allows a stair-like configuration of the oval-shaped segments to be obtained (see Fig. 5b), similar to that obtained for $Bi_{13}Ba_2Sr_{25}Fe_{13}O_{66}$ (Fig. 5c). The row of oval-shaped bismuth tapes running along $\mathbf{a}_{2201/0201}$ is brought closer to the next one by a translation $\vec{t}_a$ of $a_p/\sqrt{2}$ along $\mathbf{a}_{Bi_2Sr_4Fe_2O_{10}}$.

In other words, starting from the ideal structure of $Bi_2Sr_4Fe_2O_{10}$ (Fig. 6a), a shearing mechanism (t_c) applied along the $\vec{c}$ direction of this structure every seven bismuth atoms (see vertical arrows, Fig. 6a) allows a first, hypothetical, simple collapsed structure to be obtained (Fig. 6b); such a phenomenon does not imply any change of the formulation. In the latter structure two successive bismuth–oxygen discontinuous layers, having a stair-like configuration (see Fig. 6b), are brought closer together by a translation ($\vec{t}_a$) along $a_{2201/0201}$; this leads, by suppression of 1 FeO_6 octahedron out of 14, to the $Bi_{13}Ba_2Sr_{25}Fe_{13}O_{66}$ structure (Fig. 6c), which can then be described as a double collapsed structure with respect to the

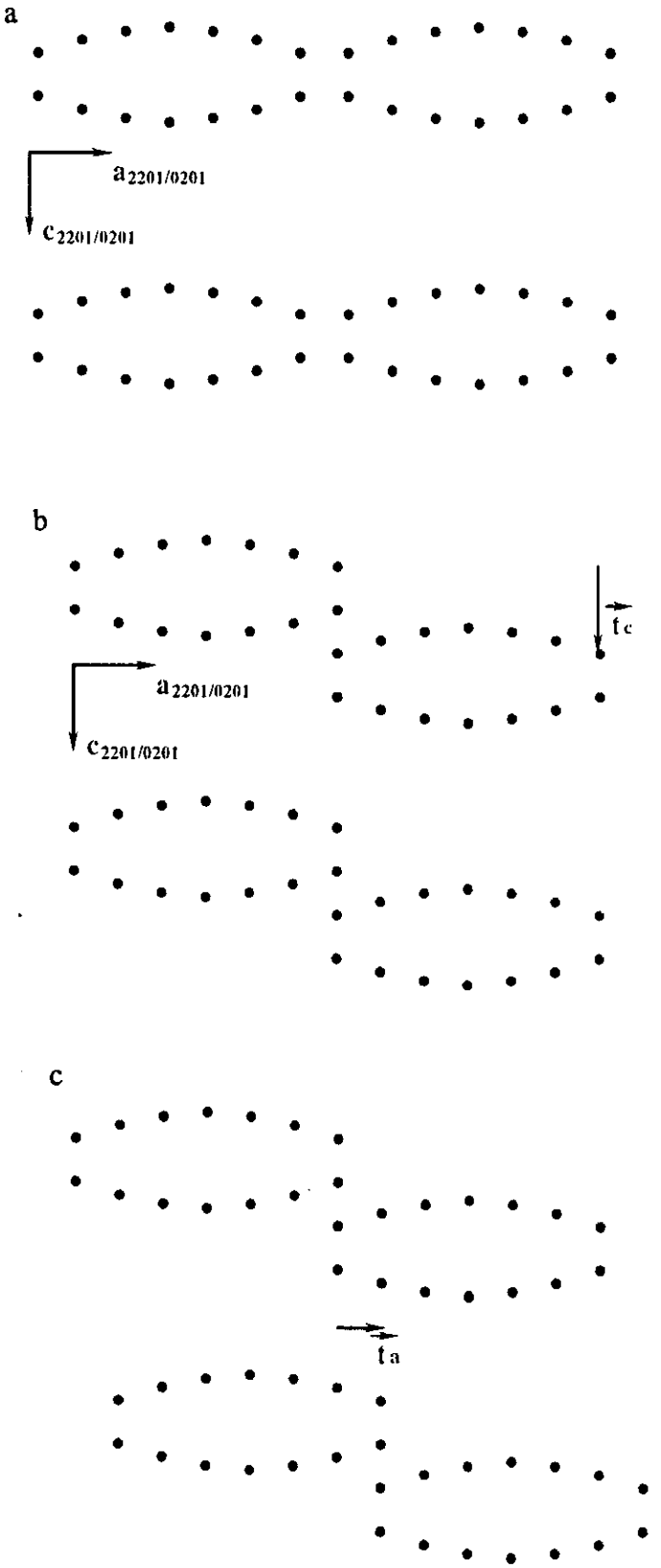

FIG. 5. Schematic representation of different relative positions of the oval-shaped segments corresponding to the double BiO tapes; only the positions of the bismuth atoms are represented (small dark points) in: (a) the 2201/0201 parent structure; (b) the hypothetical simple 2201/0201 collapsed structure, resulting from a single translation along c; and (c) the double 2201/0201 collapsed structure of $Bi_{13}Ba_2Sr_{25}Fe_{13}O_{66}$, resulting from a double translation, along c and a.

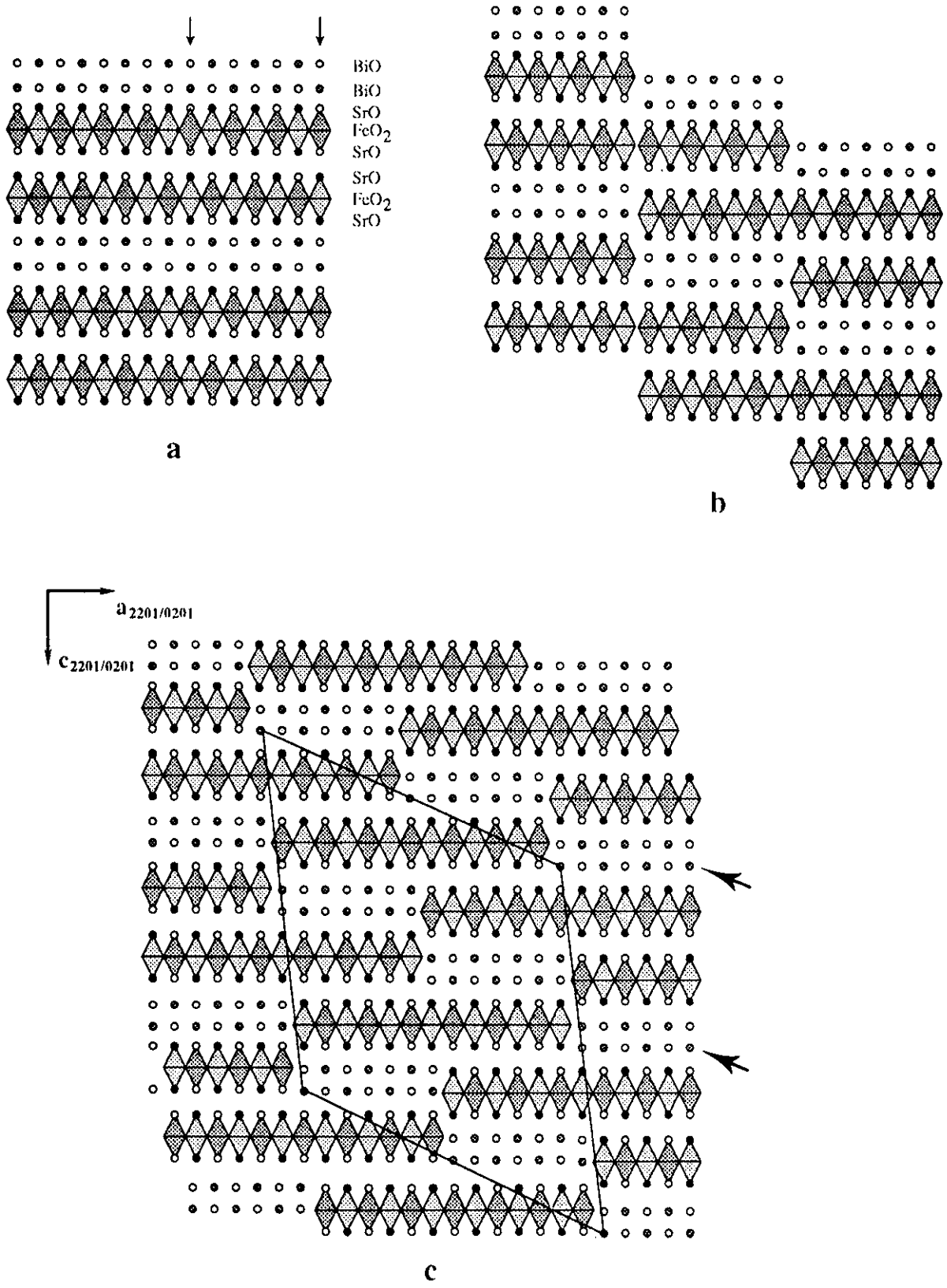

FIG. 6. Idealized structures, projected along *b*, of (a) the 2201/0201 parent structure, $Bi_2Sr_4Fe_2O_{10}$; (b) the hypothetical simple 2201/0201 collapsed structure; and (c) the double collapsed 2201/0201 structure, $Bi_{13}Ba_2Sr_{25}Fe_{13}O_{66}$.

"0201–2201" intergrowth $Bi_2Sr_4Fe_2O_{10}$. Consequently, the structure of this new double collapsed phase consists of (BiO) tapes connected to $(SrO)_{26}$ tapes on one side and to $(FeO_2)_{13}$ tapes on the other side, forming infinite layers parallel to (001) $Bi_2Sr_4Fe_2O_{10}$ according to the sequence "$(BiO)_7$–$(SrO)_{26}$–$(BiO)_7$–$(FeO_2)_{13}$."

An interesting description of the structure can be made by considering the stacking of the different (001) layers of this new structure (see oblique arrows Fig. 6c). The latter can be described as built up from stair-like bismuth–oxygen layers $[Bi_{2-x}Ba_xO_2]_\infty$, alternately stacked with K_2NiF_4-type layers that are 13 FeO_6 octahedra thick, i.e., $[(Sr'_{2-x}Ba'_xFeO_4)_{13}]_\infty$ layers. Thus the ferrite $Bi_{13}Ba_2Sr_{25}Fe_{13}O_{66}$ can be described as the $n = 13$ member of a series of oxides with the generic composition $(Bi_{2-x}Ba_xO_2)_7(Sr_{2-y}Ba_yFeO_4)_n$, which differ from each other by the thickness of the K_2NiF_4-type layers. The hypothetical single collapsed structure (Fig. 6b) corresponds to the member $n = 14$; it would exhibit a formula similar to $Bi_2Sr_4Fe_2O_{10}$. Attempts to stabilize this phase by partial substitution of barium for bismuth and for strontium were unsuccessful to date. Other kinds of collapsing every 5, 6, or 8 bismuth rows should also be considered, based on the possible existence of a large family of oxides with the general composition $(Bi_{2-x}Ba_xO_2)_m(Sr_{2-y}Ba_yFeO_4)_n$.

Note that the structural model of the structure of this phase is ideal and that the actual structure is more complex. There exists indeed an undulation of the layers due to the stereoactivity of the $6s^2$ lone pair of Bi (III) (oval-shaped segments) that has not been represented in the structural model of Fig. 6c. A second point deals with the composition, which varies slightly from one crystal to the other according to the EDX measurements in the limits "$Bi_{13\pm0.5}Ba_{2\pm0.5}Sr_{25\pm1}Fe_{13\pm1}$." This slight variation of the chemical composition is due to the presence of extended defects coherent with the matrix, but it may also result from the fact that the nature of the cations that sit at the level of the crystallographic collapsing planes is not always well defined for local substitutions such as "Bi/Fe" or "Bi/Sr," due to the "distortion" or modification of the polyhedra at the boundary. Consequently a variation of the oxygen content with respect to the ideal formula cannot be discarded.

EXTENDED DEFECTS

The overall images show that three types of extended defects which break the regularity of the collapsing mechanism are commonly observed.

Longitudinal Intergrowths of Various m Members

The stair-like (Bi_2O_2) layers are not always regular, i.e., the bismuth tapes that form such layers are not always

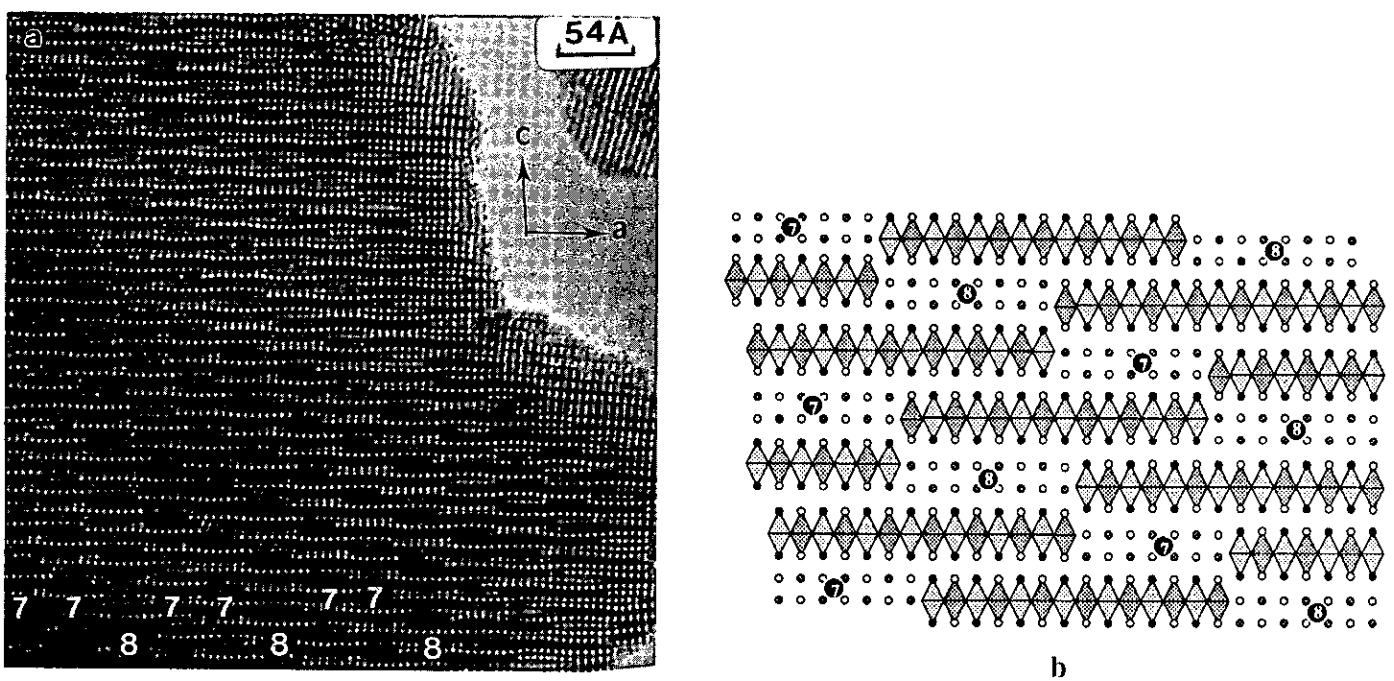

FIG. 7. (a) Enlarged [010] image of a zone where $m' = 8$ members are regularly intergrown with $m = 7$ members, involving the local formation of a $[m = 7]_2[m' = 8]_1$ new member. (b) Idealized drawing of the new complex member (the numbers of octahedra in the BiO tapes are marked in dark circles).

seven bismuth atoms wide; sometimes one observes tapes that are six or eight bismuth atoms wide. This is illustrated in Fig. 7a, where one observes $m' = 8$ tapes in a matrix of $m = 7$. The schematic structure of such a defect (Fig. 7b) shows that it can be described as a longitudinal intergrowth of the two members $m = 7$ and $m' = 8$, whereas at the level of this defect the K_2NiF_4 layers are $n = 14$ FeO_6 octahedra thick. Thus, locally such defects can be described as the longitudinal intergrowth of two members $(Bi_{2-x}Ba_xBi_2O_2)_7(Sr_{2-y}Ba_yFeO_4)_{13}$ and $(Bi_{2-x}Ba_xO_2)_8(Sr_{2-y}Ba_yFeO_4)_{15}$.

A second kind of intergrowth is observed; $m = 7$ oval-shaped bismuth segments are sometimes longitudinally intergrown either with $m' = 14$ or with $m' = 21$ bismuth segments. An example is shown in Fig. 8 (white arrowheads). These defects can be compared to the first ones except that m' is usually a multiple of the m value ($m' = 2 \times m$ or $3 \times m$), and that, in fact, two types of connections are observed between the $m = 7$ and the $m' = 14$ regions of the crystals as shown, for instance, in areas labeled 1 and 2. In area 1, the junction is parallel to (100), whereas the other one (area 2) is parallel to (101). Schematic drawings (Figs. 8b and 8c), where only the oval-shaped bismuth segments of the $m = 7$ structure and the linear bismuth segments of the $m' = 14$ are represented, show the two planes that ensure the junctions. The formation of the first type of defects $m' = 2 \times$ m (area 1) results, in fact, from the formation of antiphase boundaries (A.B.) parallel to (100) in the $m = 7$ structure; in the second type of defect (area 2), the boundary is parallel to (101) and the

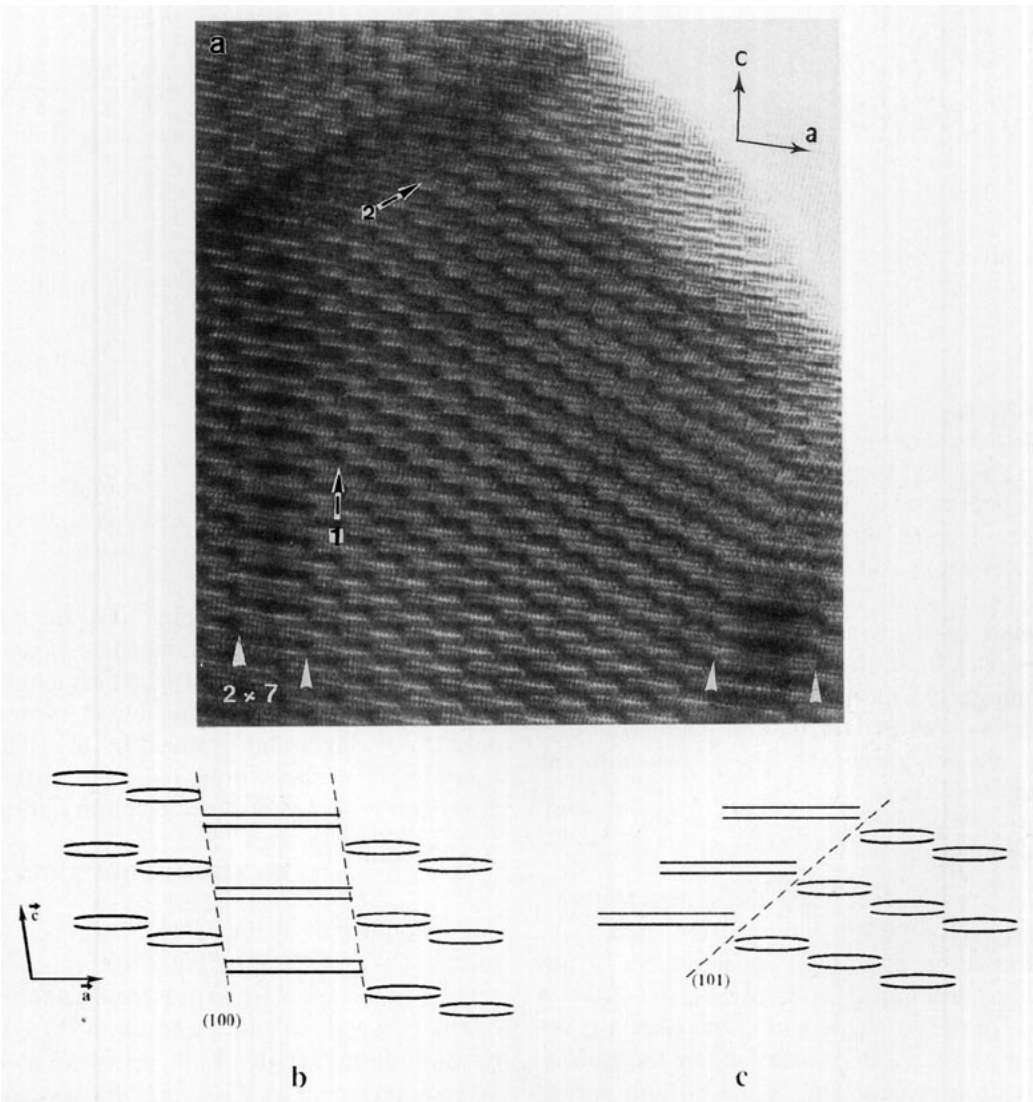

FIG. 8. (a) [010] image showing the formation of $m' = 14$ members (between the white arrowheads); the boundaries are parallel to (100) in area 1 and to (101) in area 2. The schematic drawings of the BiO tapes are given in (b) and (c), respectively.

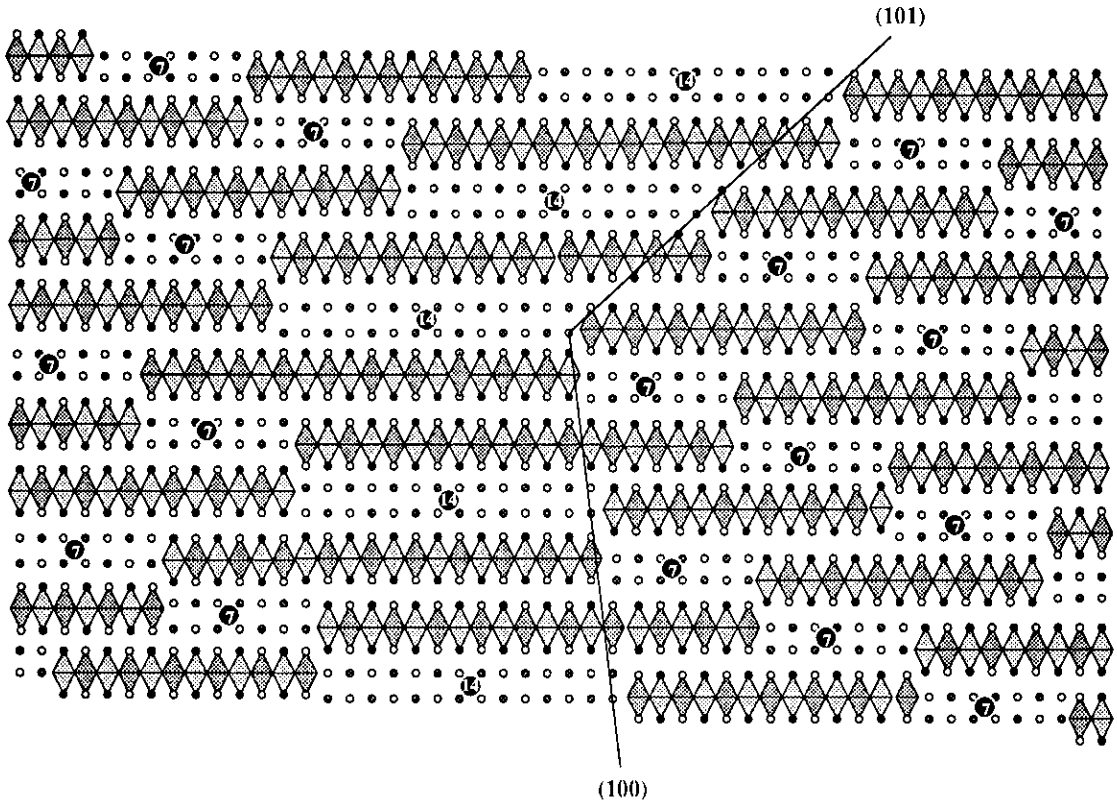

FIG. 9. Idealized structure of the new members formed through (100) and (101) boundaries.

junction between the new $m' = 14$ member and $m = 7$ matrix involves the local formation of a 2201 structure. This is easily understood by considering the idealized structure of these defects (Fig. 9) where these antiphase boundaries are represented. Considering the structure of the $m = 7$ member (Fig. 6), one can build up new slices that are 14 bismuth atoms wide, connected to the matrix through boundaries which are parallel either to (100) or to (101); then the association of such slices allows the $m' = 14$ members, with 2201/0201 and 2201 structure, respectively, to be generated and intergrown with the $m = 7$ structure.

Superdislocation

In Fig. 10, one observes two types of complex features. In the right part of the image (white arrowheads), one observes the formation of a $m' = 14$ members, a few layers thick, as a result of a A.B. parallel to (101). A regular decrease of the m' value within the ribbon is observed until one obtains a disappearance of the ribbon, in a superdislocation mechanism; in the bottom part of the image (black arrow), the $m = 7$ regular structure is restored.

Extra SrO Layers

In areas labeled S (Figs. 10a and 10b), one observes bright slices where the collapsed structure and the formation of ribbons are no longer observed. These slices are parallel to (001).

In the enlarged image (Fig. 10b), the oval-shaped bismuth segments are imaged as rows of dark dots. At the level of the defects, these typical segments are no longer observed; the through-focus series shows that, in fact, only $[SrO]_\infty$ layers are stacked in these slices. Note that similar $(SrO)_\infty$ slices or ill-crystallised (001) slices have also been reported in other bismuth cuprates (13, 14).

CONCLUDING REMARKS

The synthesis of the ferrite $Bi_{13}Ba_2Sr_{25}Fe_{13}O_{66}$ shows for the first time the possibility to create collapsed ferrites related to those obtained in bismuth cuprates. This study opens the way to the exploration of a large family of bismuth-based ferrites built up from stair-like "Bi_2O_2" layers intergrown with K_2NiF_4-type layers. The formation of complex intergrowth defects and antiphase boundaries support strongly this viewpoint.

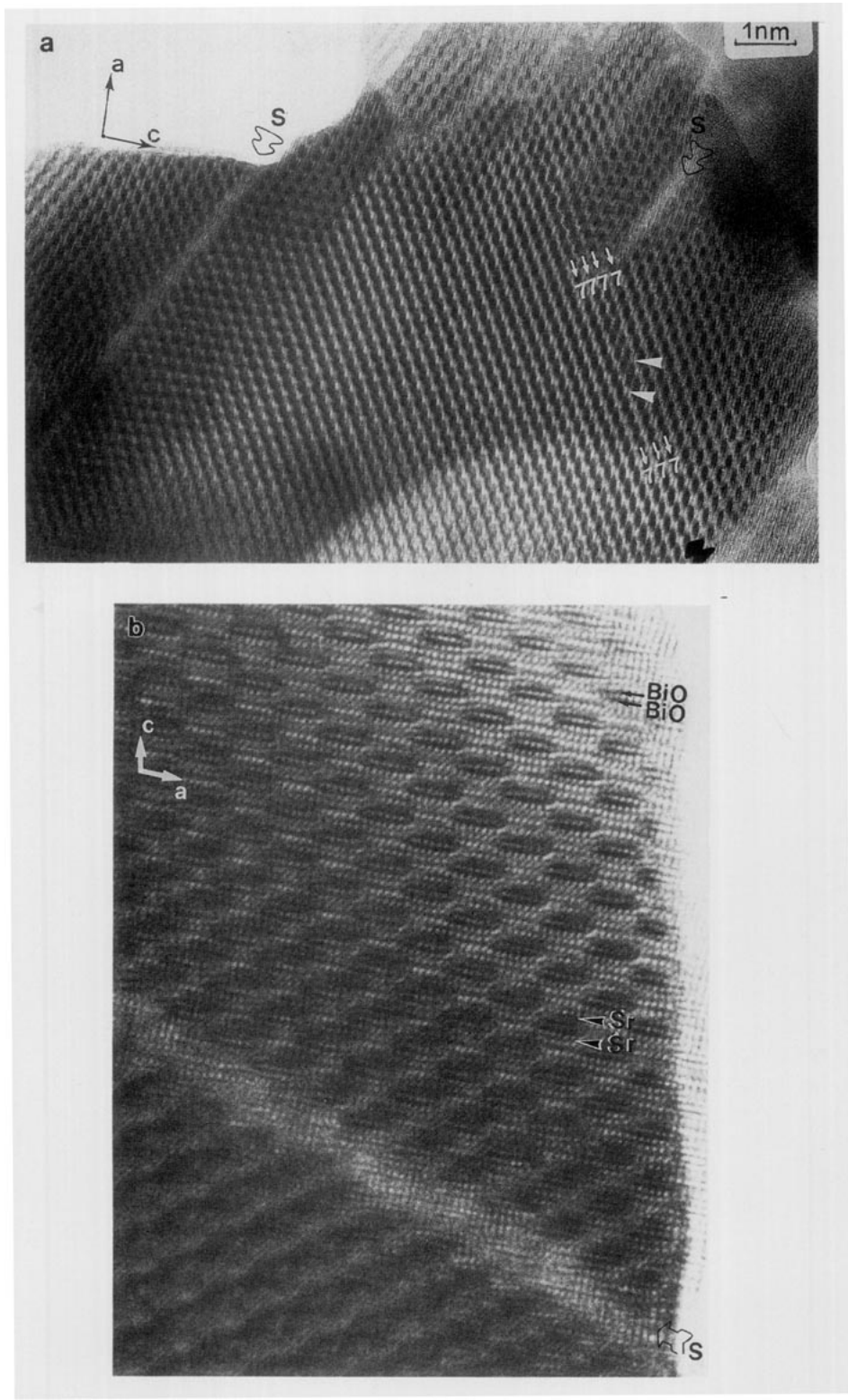

FIG. 10. [010] image where two types of defects are observed. (a) Dark arrow: large member is formed (white arrowheads) with a (101) boundary; its width regularly decreases up to $m = 7$ in a superdislocation mechanism. Open arrow S: in the slices labeled S, the collapsed structure in no longer observed. (b) Enlarged image of the defect labeled S, which consists of the existence of additional [SrO] layers.

REFERENCES

1. J. M. Tarascon, Y. Lepage, W. R. McKinnon, R. Ramesh, M. Eibschutz, E. Tselepis, E. Wang, and G. W. Hull, *Physica C* **167,** 20 (1990).
2. C. Michel, M. Hervieu, M. M. Borel, A. Grandin, F. Deslandes, J. Provost, and B. Raveau, *Z. Phys. B* **68,** 421 (1987).
3. C. C. Torardi, M. A. Subramanian, J. C. Calabrese, J. Gopalakrishnan, E. M. McCarron, K. J. Morrissey, T. R. Askew, R. B. Filippen, U. Chowdary, and A. W. Sleight, *Phys. Rev. B* **38,** 225 (1988).
4. M. Hervieu, C. Michel, N. Nguyen, R. Retoux, and B. Raveau, *Eur. J. Solid State Inorg. Chem.* **25,** 4, 375 (1988).
5. R. Retoux, C. Michel, M. Hervieu, N. Nguyen, and B. Raveau, *Solid State Comm.* **69,** 6,599 (1989).
6. H. Maeda, J. Tanaka, M. Fukutomi, and T. Asano, *Jpn. J. Appl. Phys.* **27,** L209 (1988).
7. J. M. Tarascon, W. R. McKinnon, P. Barboux, D. M. Hwang, B. G. Bagley, L. H. Greene, G. Hull, Y. Lepage, and N. Stoffel, *Phys. Rev. B* **38,** 8885, (1988).
8. M. Takano, Y. Takada, K. Oda, H. Kitaguchi, Y. Miura, Y. Ikeda, Y. Tomii, and H. Mazaki, *Jpn. J. Appl. Phys.* **27,** L1041, (1988).
9. M. Hervieu, D. Pelloquin, C. Michel, M. T. Caldes, and B. Raveau, *J. Solid State Chem.*, in press.
10. M. Hervieu, C. Michel, A. Q. Pham, and B. Raveau, *J. Solid State Chem.* **104,** 289 (1993).
11. M. Hervieu, C. Michel, M. T. Caldes, A. Q. Pham, and B. Raveau, *J. Solid State Chem.* **107,** 117 (1993).
12. J. Rodriguez-Carjaval, Proc. Satellite Meeting on Powder Diffraction of the XVth Congress of Int. Union of Crystallography, Toulouse, France, July, 1990.
13. M. Hervieu, B. Domenges, C. Michel, and B. Raveau, *Mod. Phys. Lett.* 2,835, (1988).
14. O. Eibl, *Physica C* **168,** 249 (1990).